Simulation and Realization of Free Space Optical Switch Architecture Based on MEMS Vertical Mirrors

W. J. Wang, R. M. Lin

Centre for Mechanics of Micro-Systems, School of Mechanical & Production Engineering,
Nanyang Technological University, Singapore, 639798, mwjwang@ntu.edu.sg

ABSTRACT

In this paper, we report on a novel optical cross-connect switch architecture based on MEMS vertical mirrors. The switch consists of a pair of MEMS mirror arrays to redirect optical beams from an input fiber array to an output array. Each mirror is actuated by two electrostatic comb drive actuators, and can be rotated bi-directionally and perpendicularly to the chip surface. Finite element method and Gaussian beam propagation model are used to simulate and validate the proposed optical cross-connect switch architecture. The switch concept has been demonstrated using 1550 nm single-mode optical fibers at the switch ports. Results have shown that the switch is much less constrained by the scaling distance of light propagation as the port count grows compared to previously reported switch architectures.

Keywords: MEMS, free-space, optical switch architecture, Gaussian beam optics, finite element method.

1 INTRODUCTION

Optical cross-connect switches have the potential to be a cost-effective alternative to electronic switches by avoiding optical-to-electronic and electronic-to-optical conversion. Recent advances in the field of micro-electro-mechanical systems (MEMS) have made MEMS-based optical cross-connect switches a promising technology [1]. MEMS-based optical cross-connect switches have numerous advantages including compact size, low power consumption, batch-fabrication, and fast switching speed. In this paper, we present a novel optical cross-connect switch architecture that has the potential to be scaled to large numbers of port counts, while low crosstalk and insertion loss are maintained.

2 DESIGN OF OPTICAL SWITCH

Two micro-mirror arrays, including input mirror array and output mirror array, establish an optical path between the input and output optical ports. The input mirror array directs each input optical beam to the designed output mirror array, and the output mirror array aligns the optical beams for coupling into the output fibers. The mirror rotational axes lie in the center of each mirror, and the mirror centers are collinear in both arrays. The input and output optical fibers (1550 nm single-mode) are placed in etched silicon grooves.

2.1 Micro-Mirrors

The micro-mirror is rectangular and the optical surface is 150 μm in height by 150 μm in length. The mirror is supported by two crab-flexures (as shown in Figure 1), which are in turn mounted on two anchors fixed to the substrate. The crab-flexures are used provide sufficient flexibility for large mirror deformation. The dimensional parameters and values are listed in Table 1.

It is desirable to have smooth surface for the micro-mirrors in order to minimize scattering caused by mirror surface roughness. Moreover, any curvature of the micro-mirrors affects the coupling efficiency dramatically for free-space MEMS optical switches. Using MEMS

technologies, means to avoid deformations can include: 1) planarization methods such as chemical-mechanical polishing (CMP) to make flat, thin-film mirrors [2], and 2) using bulk micromachining to produce a flat, single-crystal silicon mirror [3]. Here, bulk-micromachined thicker single-crystal silicon mirrors are used for the optical switching.

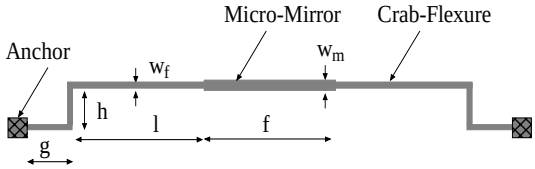

Figure 1: Schematic drawing of the micro-mirror and crab-flexures.

Table 1: Design parameters of micro-mirror and flexures

	Description	Value (μm)
w_f	Width of flexures	3
w_m	Width of micro-mirrors	6
f	Length of micro-mirrors	150
g	Length of connector	40
h	Length of thigh	40
l	Length of the beams	200

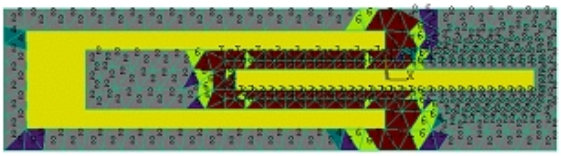

Figure 2: The mesh elements for the electrostatic comb drive with one set of fingers

Finite element calculations are performed using commercial finite-element program, ANSYS. The micro-mirror and crab-flexures are modeled using three-dimensional shell element. The p-method is used for the electrostatic analysis during the simulation. The mesh elements for the electrostatic comb drive with one set of fingers can be seen in Figure 2. For 60 V voltage, the mirror rotation angle is about 13°.

2.2 Switch Architecture

The size and angular deflection range of the micro-mirrors, and the optics of the switches limit the scaling of the proposed optical switch architecture. Here, Gaussian beam optics is used to analyze the scalability of the proposed optical switch architecture. The complex amplitude $U(\vec{r})$ of a paraxial Gaussian-beam can be expressed as [4],

$$U(\vec{r}=(x,y,z)) = A_0\left\{\frac{w_0}{w(z)}\exp\left[-\frac{\rho^2}{w^2(z)}\right]\right\}\ \text{amplitude factor}$$
$$\times\exp\left[-j\frac{k\rho^2}{2R(z)}\right]\ \text{radial phase} \qquad (1)$$
$$\times\exp\left[-jkz + j\tan^{-1}\left(\frac{z}{z_R}\right)\right]\ \text{longitudinal factor}$$

where

A_0 a constant;

z propagation direction of the Gaussian-beam;

ρ radial distance from the axis of the beam;

k wavenumber, where λ is the wavelength;

w_0 $1/e$ half-width at beam waist;

z_R a parameter (Rayleigh range) defined as,

$$z_R = \frac{\pi w_0^2}{\lambda} \qquad (2)$$

for free space. The divergence of the optical beam results in an increase of the $1/e$ half-width $w(z)$ with z given by,

$$W(z) = W_0\sqrt{1+\left(\frac{z}{z_R}\right)^2} \qquad (3)$$

and yields a curved wavefront whose radius is represented by,

$$R(z) = z\left[1+\left(\frac{z_R}{z}\right)^2\right] \qquad (4)$$

According to Gaussian beam optics, for a given value of λ, variations of beam diameter and divergence with distance z are functions of a single parameter. This is often chosen to be w_0, the beam waist radius. Typically, one can calculate the beam radius $w(z)$ for a value of the light

propagation distance z according equation (3). One can also find the general expression for the optimum starting beam radius for a given distance, z,

$$w_{0(\text{opt})} = \left(\frac{\lambda z}{\pi}\right)^{1/2} \tag{5}$$

Using this optimum value of w_0 will provide the best combination of minimum starting beam diameter and minimum beam spread over the distance z. If we put this optimum value for w_0 back into equation (3) for $w(z)$, $w(z) = \sqrt{2}w_0$. This result allows us to adjust the position of the beam waist so that we can actually double the distance over which beam divergence is minimized. By focusing the beam-expanding optics to place the beam waist at the midpoint, we can restrict beam spread to a factor of $\sqrt{2}$ over a distance of $2z_R$, as opposed to just z_R.

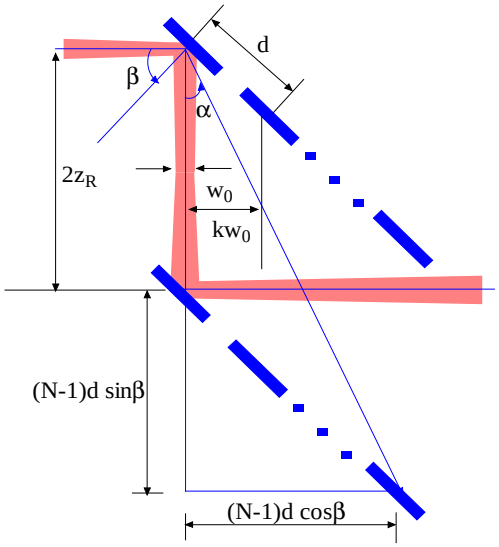

Figure 3: Gaussian beam propagation through the optical switch.

Figure 3 shows Gaussian optical beam propagation through the switch. The optical beam waist is centrally located between the micro-mirror arrays to create a symmetric switch that minimizes micro-mirror size. The optimum value of the separation between the two micro-mirror arrays is two-folds of the Rayleigh length of the optical beam, $2z_R$. The distance d between the micro-mirror centers depend on the size of the micro-mirror and the separation between adjacent optical ports which can be measured in beam waist radii, kw_0 ($k = 3 \sim 5$), as shown in Figure 3. To maxmize the separation between the micro-mirror arrays, Gaussian beams with larger beam diameters are needed. Moreover, Gaussian beams with larger beam diameters exhibit smaller divergence angles. However, the mirror size would be required to increase with beam diameter. As a result, the propagation distance of the optical beam also increases for a given device port-count. In particular, the distance between the micro-mirror centers is geometrically related to the size of micro-mirrors, and would be required to increase to minimize the crosstalk.

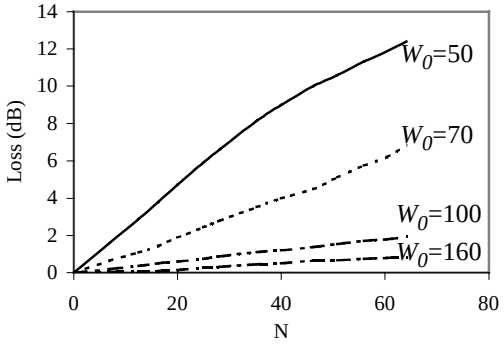

Figure 4: Theoretical studies on loss versus propagation distance with various beam waist for free space MEMS optical switches for $\gamma = \sqrt{2}$.

From above analysis, it is clear that the optimal size of the Gaussian beam will represent a compromise among these competing factors. It is useful to define a new variable given by the ratio of the size of the micro-mirror divided by the beam waist. Thus, the dimensionless quantity $s/w_0 = \gamma$, is a variable that can be optimized depending on the value of w_0. Here, we mainly emphasize the dependence of loss on optical beam size. The coupling efficiency η can be obtained by computing the normalized overlap integral of the divergent Gaussian beam wave function at the receiver plane and the nodal wave function of the receiving optics. Here, we restrict ourselves to the situation of primary interest, in which both the emitting optics and the receiving

optics are identical, with only fundamental propagating modes. Without angular misalignment, η is expressed as:

$$\eta = \frac{\left|\int U^*(x,y,z=d)\cdot U(x,y,z=0)\right|^2}{\left|U(x,y,z=d)\right|^2 \cdot \left|U(x,y,z=0)\right|^2} \qquad (6)$$

where the integral is taken over the aperture of the receiving optics. Figure 4 shows the simulation results for various beam sizes for $\gamma = \sqrt{2}$. From Figure 4, one can see that for our design the loss can be below 2 dB even if $N = 64$ for $w_0 = 100$ μm. Therefore, Gaussian beam with $w_0 = 100$ μm will be used in our design.

3 FABRICATION AND RESULTS

Fabrication starts with a photolithography on Silicon-on-Oxide (SOI) wafers to define the structure including the mirrors, alignment grooves, actuators and crab-flexures. The key fabrication step is the vertical deep reactive ion etching (DRIE) of the 150 μm device layer. In our structure, we have to open 125 μm wide trenches for the optical fiber and at the same time small gaps for the comb drive actuator. After the DRIE the photoresist is stripped. To free the mechanical structures the sacrificial silicon dioxide layer is etched in hydrofluoric acid. After the sacrificial layer etching aluminum is sputtered, patterned and etched to form the electric pad.

Figure 5: Micrograph of Al-coated surface of Si micro-mirror

To increase the reflectivity of the vertical mirrors, the silicon is metal coated. This is done by e-beam evaporation, where the wafers are oriented in an appropriate direction. Figure 5 shows a micrograph of the Al-coated surface of Si micro-mirror. The RMS surface roughness is about 36 nm.

The dependence of mirror rotation on applied voltage is shown in Figure 6. It can be seen from Figure 6 that the mirror rotation angle about 13° can be achieved using only 60 V. Therefore, the micro-mirror can be used to deflect an optical beam by 26° when 60 V voltage is applied. This angular range and mirror quality support scaling to above 32 by 32 fiber ports.

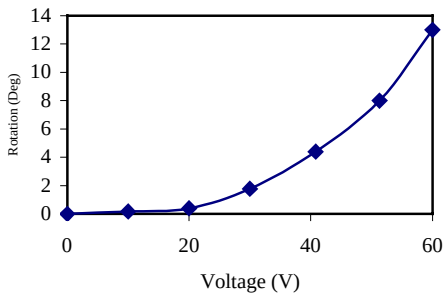

Figure 6: Micro-mirror rotation angle as a function of applied dc voltage.

REFERENCES

[1] H. Toshiyoshi and H. Fujita, “Electrostatic micro torsion mirrors for an optical switch matrix,” J. Microelectromechal System, 5, 231–237, 1996.

[2] D. L. Hetherington and J. J. Sniegowski, "Improved polysilicon surface-micromachined micromirror devices using chemical-mechanical polishing," Proc. SPIE, 3440, 148-153, 1997.

[3] S. Kurth, R. Hahn, C. Kaufmann, K. Kehr, J. Mehner, U. Wollmann, W. Dotzel, and T. Gessner, "Silicon mirrors and micromirror arrays for spatial laser beam modulation," Sensors & Actuators A (Physical), A66, 1-3, 76-82, 1998.

[4] B.E.A Saleh and M.C. Teich, Fundamentals of Photonics, John Wiley &Sons, 1991.